

Article

Single-Longitudinal-Mode Laser at 1123 nm Based on a Twisted-Mode Cavity

Yang Liu, Sasa Zhang, Zhenhua Cong, Shaojie Men , Chen Guan, Yongyao Xie and Zhaojun Liu *

School of Information Science & Engineering and Shandong Provincial Key Laboratory of Laser Technology and Application, Shandong University, Qingdao 266237, China; liuyang0301@sdu.edu.cn (Y.L.); sasazhang@sdu.edu.cn (S.Z.); zhenhuacong@sdu.edu.cn (Z.C.); shaojiemen@sdu.edu.cn (S.M.); 18253163822@163.com (C.G.); yongyxie@163.com (Y.X.)

* Correspondence: zhaojunliu@sdu.edu.cn

Abstract: A single-longitudinal-mode (SLM) Neodymium-doped Yttrium Aluminium Garnet (Nd:YAG) laser at 1123 nm was first demonstrated with a twisted-mode (TM) cavity. By eliminating the spatial hole burning phenomenon, a stable SLM 1123 nm laser output was obtained. An efficient TM cavity was designed based on the Brewster plate with high reflection under s-polarization radiation. At an incident pump power of 7.65 W, the maximum output power of 689 mW was obtained. The corresponding optical conversion efficiency was about 9%. The center wavelength was 1122.58 nm and the line-width was <140 MHz.

Keywords: 1123 nm radiation; single longitudinal mode; twisted mode cavity; high efficiency



Citation: Liu, Y.; Zhang, S.; Cong, Z.; Men, S.; Guan, C.; Xie, Y.; Liu, Z. Single-Longitudinal-Mode Laser at 1123 nm Based on a Twisted-Mode Cavity. *Crystals* **2021**, *11*, 58. <https://doi.org/10.3390/cryst11010058>

Received: 18 December 2020

Accepted: 12 January 2021

Published: 13 January 2021

Publisher's Note: MDPI stays neutral with regard to jurisdictional claims in published maps and institutional affiliations.



Copyright: © 2021 by the authors. Licensee MDPI, Basel, Switzerland. This article is an open access article distributed under the terms and conditions of the Creative Commons Attribution (CC BY) license (<https://creativecommons.org/licenses/by/4.0/>).

1. Introduction

Owing to the single-longitudinal-mode (SLM) characteristic, single-frequency lasers have many distinctive applications in detection, medicine and cold atom physics [1–4]. In addition, single-frequency lasers also play an indispensable role in many emerging scientific research works [5–7]. Therefore, single-frequency lasers have attracted intense attention and have been widely researched [8–16]. Recently, the SLM 1123 nm laser attracted the attention of our research group because it can motivate thulium up-conversion fiber lasers to produce blue laser emission [17]. Furthermore, a single-frequency yellow–green laser with a wavelength of 561 nm (second-harmonic radiation of a 1123 nm laser) has been considered the ideal source for confocal microscopy flow cytometry and other bioimaging applications [18]. It is also optimal for the treatment of complex ophthalmic diseases and has wide applications in biomedical applications [19]. To date, Neodymium-doped Yttrium Aluminium Garnet (Nd:YAG) lasers operating in the Stark component of the $4F^{3/2}-4I^{11/2}$ transition have been proven to be a practical approach to generate 1123 nm lasers [20–25]. However, since the stimulated emission cross-section for the 1123 nm transition is approximately 15 times smaller than that for the 1064 nm line [26], research into SLM 1123 nm lasers has been scarce and is almost based on ring cavity technology. In 1999, the first SLM 1123 nm laser was reported by Moore et al. with a ring cavity [20]. An output power of 180 mW was obtained at an incident pump power of 5.6 W. In 2007, with a monolithic nonplanar ring cavity, Zang et al. enhanced the output power of the SLM 1123 nm laser to 1.25 W [21]. However, the typical ring cavity always requires expensive elements such as an isolator, and in the monolithic nonplanar ring cavity, the special design and machining of the gain medium is inevitable. Compared with ring cavity technology, twisted-mode (TM) cavity technology is simpler and has a lower cost. In this technology, a pair of quarter-wave plates (QWPs) on both sides of the gain medium and a polarization beamsplitter plate (PBP) in front of the output mirror are used to control the polarization state of the intra-cavity beam. The function of the QWPs is to keep the forward-propagation beam and backward-propagation beam circularly polarized and orthogonally oriented in the gain medium. According to [8], the total energy density is

spatially uniform along the gain medium in this case; thus, there is no spatial hole burning along the gain medium and the laser can be operated in single-longitudinal mode. However, to our best knowledge, no research on an SLM 1123 nm laser based on TM cavity technology has been reported.

The typical TM cavity has a linear structure, and in 2011, Gao et al. designed an L-type cavity and increased the output power of a 2 μm SLM laser from 514 mW to 1.46 W [27]. In this work, a typical linear TM cavity and an L-type TM cavity were both used to generate an SLM 1123 nm output. A 1 at.% Nd-doped Nd:YAG crystal was selected as the gain medium. The results indicated that the L-type TM cavity showed better performance. At an incident pump power of 7.65 W, the maximum output power of 689 mW was obtained with a corresponding optical conversion efficiency of 9%. The center wavelength and line-width were 1122.58 nm and <140 MHz, respectively. The beam quality factors (M^2) in horizontal and vertical directions were 1.58 and 1.41, respectively. The polarization ratio was measured to be >650:1. To the best of our knowledge, this was the first time that the SLM laser at 1123 nm was reported with a TM cavity.

2. Experimental Setup

The experimental setup of the SLM 1123 nm lasers is shown in Figure 1. A homemade continuous-wave (CW) fiber-coupled laser diode (LD) with a fiber core diameter of 400 μm and a numerical aperture of 0.22 was used as the pump source. The output beam of the LD was re-imaged by the coupling lens (CL) into the laser crystal. The re-imaging ratio was 1:1.5. The TM cavity consisted of two cavity mirrors, two QWPs and a PBP (PBP 1150-780, Union Optics, China). The rear mirror M1 was a plane mirror. The entrance surface was coated for anti-reflection (AR) at 808 nm ($R < 0.2\%$). The other surface was coated for high reflection (HR) at 1123 nm ($R > 99.8\%$) and AR at 808 nm ($R < 0.2\%$). A pair of zero-order QWPs (QWP1 and QWP2) at 1123 nm were placed on each side of the Nd:YAG crystal. The principal axes of the QWPs were oriented with their fast axes perpendicular to each other and at 45° to the oscillating polarization direction. An Nd:YAG crystal with 1 at.% Nd-doped and dimensions of $\Phi 5 \text{ mm} \times 8 \text{ mm}$ served as the gain medium. The Nd:YAG crystal was water-cooled with the temperature maintained at 18°C . One PBP was placed at Brewster's angle behind QWP2. The output coupler (OC) M2 was also a plane mirror with a transmission of 2% at 1123 nm, of 5% at 1112 nm and of 4% at 1116 nm and high transmission (HT) at 1064 nm and 1319 nm, as shown in the inset of Figure 3. Two cavity configurations were used in the experiments. The linear TM cavity, as shown in Figure 1a, was based on the PBP with HT under p -polarization radiation. The L-type TM cavity, as shown in Figure 1b, was based on the PBP with HR under s -polarization radiation. Both cavity lengths of the two configurations were about 70 mm.

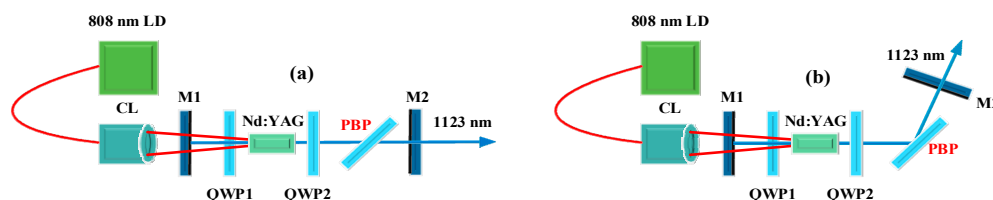


Figure 1. The experimental setup of the single-longitudinal-mode (SLM) 1123 nm lasers, (a) linear twisted-mode (TM) cavity, (b) L-type TM cavity. LD, laser diode; CL, coupling lens; QWP, quarter wave plate; PBP, polarization beamsplitter plate.

3. Experimental Results and Discussions

To begin with, we compared the output power of the two TM cavities versus the incident pump power, and the results are shown in Figure 2. The output power was measured by a power meter (PM10, Molectron, America) connected to a Molectron device (EPM2000, Molectron, America). For the linear TM cavity, the threshold pump power was 4.57 W. The output power increased linearly with the incident pump power, and the slope

efficiency was about 11%. At an incident pump power of 8.9 W, the maximum output power of 497 mW was obtained. With an L-type TM cavity, the threshold was 3.4 W lower than that in a linear TM cavity, and a higher output power and slope efficiency were obtained. At an incident pump power of 7.65 W, the output power was measured to be 689 mW. The slope efficiency was 16%, which was 5% higher than that in the linear TM cavity. The better performance of the L-type TM cavity was mainly due to the commercial PBP with a transmission of >95% under *p*-polarization radiation and a reflection of >99% under *s*-polarization radiation. With the laser with an L-type cavity (*s*-polarization radiation oscillation), the loss of the cavity was reduced. Thus, the threshold value was decreased and the optical conversion efficiency was improved. For the same reason, in order to ensure the output laser was always in single-longitudinal mode, the maximum pump power in the L-type cavity was lower than that in linear cavity. In addition, the transmission of the OC was not optimal. In future work, if the transmission of the OC can be optimized, we believe that the output power and the slope efficiency could be further improved.

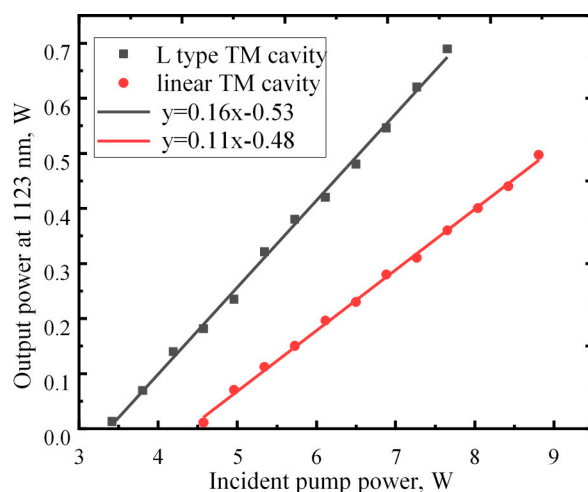


Figure 2. The average output power of the 1123 nm laser versus the incident pump power.

In the following experiments, all the results were measured at an incident pump power of 7.65 W with an L-type TM cavity. The laser emission spectrum was observed with a wide-range optical spectrum analyzer (AQ6315A, Yokogawa, Japan). The wavelength span and scanning resolution were set to 1000–1500 nm and 0.5 nm, respectively. As shown in Figure 3, only one laser line located at 1123 nm was observed. The HT coatings at 1064 nm and 1319 nm effectively suppressed the oscillations of these two wavelengths with high gain. In addition, although the emission cross sections at 1112 nm, 1116 nm and 1123 nm were similar in the Nd:YAG crystal [28], the transmissions at 1112 nm and 1116 nm of the OC were higher than at 1123 nm. Therefore, the laser lines at 1112 nm and 1116 nm did not oscillate. The transmission curve as a function of wavelength for the OC is given in the inset of Figure 3.

The longitudinal mode characteristic and line width were measured with a wavelength meter (WS-7, Highfinesse, Germany). The resolution of the wavelength meter was 10 MHz. The results are shown in Figure 4. The center wavelength was 1122.58 nm in a vacuum and the line width was less than 0.6 pm (<140 MHz). Considering the refractive index of the crystal and PBP, the effective cavity length was about 80 mm. As a result, the longitudinal mode interval could be calculated to be ~1.87 GHz [29]. The line width was much lower than the cavity's longitudinal mode interval, and there was only one set of interference patterns, as shown in Figure 4. All the data illustrate that the TM laser was operating in single-longitudinal mode.

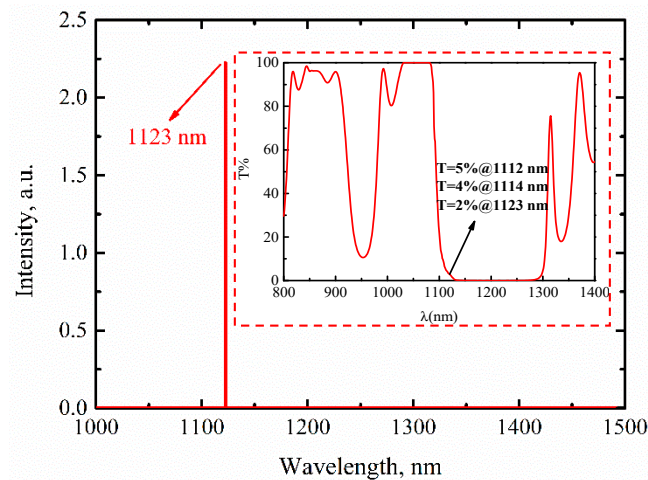


Figure 3. The output spectrum of the L-type TM cavity laser. The inset shows the transmission curve as a function of wavelength for the output coupler (OC).

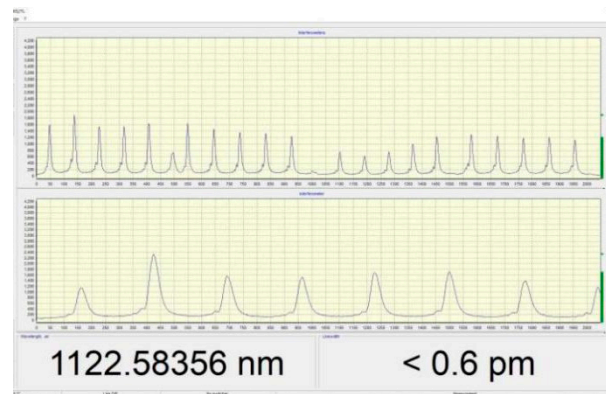


Figure 4. The longitudinal mode characteristic of the 1123 nm laser at 7.65 W incident pump power.

With an incident pump power of 7.65 W, we also measured the polarization characteristic and M^2 of the SLM 1123 nm laser. By using a half-wave plate (HWP) and a PBP, we measured the polarization characteristics. Figure 5 shows the power behind the PBP as a function of the HWP's rotation angle. The maximum power and minimum power were 650 mW and <1 mW, respectively. The total power before the PBP was about 680 mW. The measurement results indicated that the transmissions of PBP at p -polarization and s -polarization were >95% and <0.14%, respectively. Thus, the actual extinction ratio could be calculated to be >678:1 and the polarization ratio of the SLM 1123 nm laser was >650:1. The M^2 measurement was performed by focusing the beam of the 1123 nm laser onto a charge coupled device (CCD) camera by using a biconvex lens ($f = 100$ mm). By measuring the laser spot radius and fitting the experimental results, we could calculate the M^2 of the 1123 nm laser. As shown in Figure 6, the values of M^2 in horizontal and vertical directions were 1.58 and 1.41, respectively.

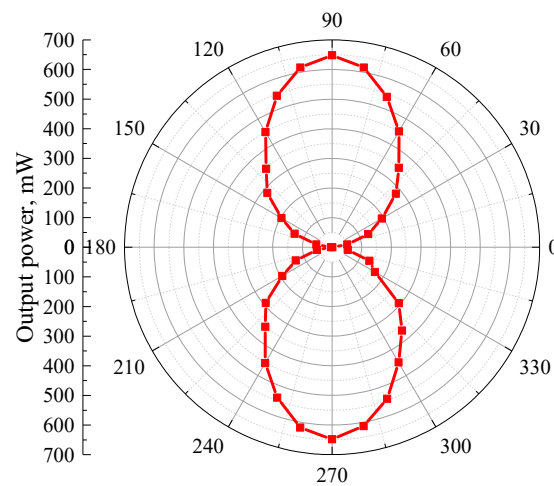


Figure 5. The polarization characteristic of the SLM 1123 nm laser at 7.65 W incident pump power.

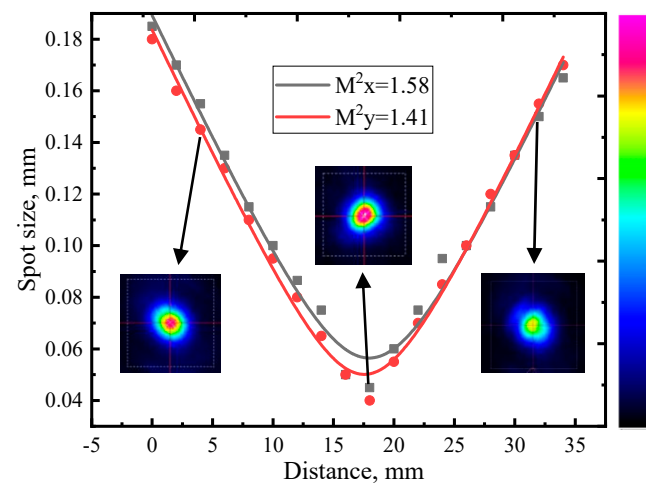


Figure 6. The beam quality of the SLM 1123 nm laser at 7.65 W incident pump power. The insets show the laser spot of the 1123 nm laser at different positions.

4. Conclusions

In summary, SLM 1123 nm laser emission has been realized by eliminating the spatial hole burning phenomenon. An efficient TM cavity was designed based on the Brewster plate with high reflection under *s*-polarization radiation. The center wavelength was 1122.58 nm, and the line width was <140 MHz. The maximum output power of 689 mW was obtained under an incident pump power of 7.65 W. The slope efficiency was 16%. In addition, the polarization ratio of the SLM 1123nm laser was >650:1 and the M^2 values in horizontal and vertical directions were 1.58 and 1.41, respectively. To the best of our knowledge, this is the first time that the SLM laser at 1123 nm was reported with a TM cavity. In the future, we will undertake more research on the TM cavity SLM 1123 nm laser to improve the output performance, such as optimizing the transmissions of the OC, optimizing the selection of the gain medium (Nd-doped concentration, length, category), optimizing the pump source (spectral width, spot size on the gain medium) and inserting etalons or gratings in the cavity to further compress the line width.

Author Contributions: Conceptualization, Y.L.; methodology, Y.L.; validation, Y.L. and C.G.; formal analysis, S.Z.; investigation, Y.L.; resources, Z.L.; data curation, Y.X.; writing—original draft preparation, Y.L.; writing—review and editing, Z.L. and S.M.; funding acquisition, Z.L. and Z.C. All authors have read and agreed to the published version of the manuscript.

Funding: This research was funded by the Natural Science Foundation of China, grant number 62075117 and 62075116, Joint Foundation of the Ministry of Education, grant number 6141A02022430, Natural Science Foundation of Shandong Province, grant number ZR2019MF039.

Conflicts of Interest: The authors declare no conflict of interest.

References

1. Sane, S.S.; Bennetts, S.; Debs, J.E.; Kuhn, C.C.N.; McDonald, G.D.; Altin, P.A.; Close, J.D.; Robins, N.P. 11 W narrow linewidth laser source at 780 nm for laser cooling and manipulation of Rubidium. *Opt. Express* **2012**, *20*, 8915–8919. [[CrossRef](#)] [[PubMed](#)]
2. Kuhn, V.; Kracht, D.; Neumann, J.; Wessels, P. Er-doped single-frequency photonic crystal fiber amplifier with 70 W of output power for gravitational wave detection. In *Fiber Lasers IX: Technology, Systems, and Applications*; SPIE 8237; SPIE: San Francisco, CA, USA, 2012.
3. Wu, T.; Peng, X.; Gong, W.; Zhan, Y.Z.; Lin, Z.S.; Luo, B.; Guo, H. Observation and optimization of He⁻⁴ atomic polarization spectroscopy. *Opt. Lett.* **2013**, *38*, 986–988. [[CrossRef](#)] [[PubMed](#)]
4. Canat, G.; Augere, B.; Besson, C.; Dolfi-Bouteyre, A.; Durecu, A.; Goular, D.; Gouet, J.L.; Lombard, L.; Planchat, C.; Valla, M. High peak power single-frequency MOPFA for lidar applications. In Proceedings of the 2016 Conference on Lasers and Electro-Optics (CLEO), San Jose, CA, USA, 5–10 June 2016.
5. Zhang, Q.; Hou, Y.B.; Wang, X.; Song, W.H.; Chen, X.; Bin, W.; Li, J.; Zhao, C.N.; Wang, P. 5 W ultra-low-noise 2 μm single-frequency fiber laser for next-generation gravitational wave detectors. *Opt. Lett.* **2020**, *45*, 4911–4914. [[CrossRef](#)]
6. Wang, K.X.; Gao, C.Q.; Lin, Z.F.; Wang, Q.; Gao, M.W.; Huang, S.; Chen, C.Y. 1645 nm coherent Doppler wind lidar with a single-frequency Er:YAG laser. *Opt. Express* **2020**, *28*, 14694–14704. [[CrossRef](#)] [[PubMed](#)]
7. Sonnenschein, V.; Tomita, H.; Kotaro, K.; Koya, H.; Studer, D.; Terabayashi, R.; Weber, F.; Wendt, K.; Nishizawa, N.; Iguchi, T. A direct diode pumped Ti:sapphire laser with single-frequency operation for high resolution spectroscopy. *Hyperfine Interact* **2020**, *241*, 32. [[CrossRef](#)]
8. Evtuhov, V.; Siegman, A.E. A Twisted-Mode Technique for Obtaining Axially Uniform Energy Density in Laser Cavity. *Appl. Opt.* **1965**, *4*, 142–143. [[CrossRef](#)]
9. Wu, E.; Pan, H.; Zhang, S.; Zeng, H. High power single-longitudinal-mode operation in a twisted-mode-cavity laser with a c-cut Nd:GdVO₄ crystal. *Appl. Phys. B-Lasers O* **2005**, *80*, 459–462. [[CrossRef](#)]
10. Zhang, Y.; Gao, C.; Gao, M.; Lin, Z.; Wang, R. A diode pumped tunable single-frequency Tm:YAG laser using twisted-mode technique. *Laser Phys. Lett.* **2010**, *7*, 17–20. [[CrossRef](#)]
11. Kane, T.J.; Byer, R.L. Monolithic, Unidirectional Single-Mode Nd:YAG Ring Laser. *Opt. Lett.* **1985**, *10*, 65–67. [[CrossRef](#)] [[PubMed](#)]
12. Wang, L.; Gao, C.Q.; Gao, M.W.; Li, Y. Resonantly pumped monolithic nonplanar Ho:YAG ring laser with high-power single-frequency laser output at 2122 nm. *Opt. Express* **2013**, *21*, 9541–9546. [[CrossRef](#)] [[PubMed](#)]
13. Wu, C.T.; Ju, Y.L.; Wang, Z.G.; Wang, Q.; Song, C.W.; Wang, Y.Z. Diode-pumped single frequency Tm:YAG laser at room temperature. *Laser Phys. Lett.* **2008**, *5*, 793–796. [[CrossRef](#)]
14. Lin, Z.; Gao, C.; Gao, M.; Zhang, Y.; Weber, H. Diode-pumped single-frequency microchip CTH:YAG lasers using different pump spot diameters. *Appl. Phys. B Lasers O* **2009**, *94*, 81–84. [[CrossRef](#)]
15. Pedersen, C.; Hansen, P.L.; Skettrup, T.; Buchhave, P. Diode-Pumped Single-Frequency Nd:YVO₄ Laser with a Set of Coupled Resonators. *Opt. Lett.* **1995**, *20*, 1389–1391. [[CrossRef](#)] [[PubMed](#)]
16. Wu, C.T.; Ju, Y.L.; Wang, Z.G.; Li, Y.F.; Ma, H.Y.; Wang, Y.Z. Lasing characteristics of a CWTm: LuAG laser with a set of double cavity. *Laser Phys. Lett.* **2008**, *5*, 510–513. [[CrossRef](#)]
17. Paschotta, R.; Moore, N.; Clarkson, W.A.; Tropper, A.C.; Hanna, D.C.; Maze, G. 230 mW of blue light from a thulium-doped upconversion fiber laser. *IEEE J. Sel. Top Quant.* **1997**, *3*, 1100–1102. [[CrossRef](#)]
18. Telford, W.; Murga, M.; Hawley, T.; Hawley, R.; Packard, B.; Komoriya, A.; Haas, F.; Hubert, C. DPSS yellow-green 561-nm lasers for improved fluorochrome detection by flow cytometry. *Cytom. Part A* **2005**, *68*, 36–44. [[CrossRef](#)] [[PubMed](#)]
19. Gao, J.; Dai, X.J.; Zhang, L.; Sun, H.X.; Wu, X.D. A Continuous-Wave Medical Yellow Laser at 561 nm. In Proceedings of the Conference on Lasers and Electro-Optics Europe and International Quantum Electronics Conference, Munich, Germany, 12–16 May 2013.
20. Moore, N.; Clarkson, W.A.; Hanna, D.C.; Lehmann, S.; Bosenberg, J. Efficient operation of a diode-bar-pumped Nd:YAG laser on the low-gain 1123-nm line. *Appl. Opt.* **1999**, *38*, 5761–5764. [[CrossRef](#)] [[PubMed](#)]
21. Zang, E.J.; Cao, J.P.; Li, Y.; Yang, T.; Hong, D.M. Single-frequency 1.25 W monolithic lasers at 1123 nm. *Opt. Lett.* **2007**, *32*, 250–252. [[CrossRef](#)]
22. Li, P.; Chen, X.H.; Zhang, H.N.; Ma, B.M.; Wang, Q.P. Diode-Pumped Passively Q-Switched Nd:YAG Ceramic Laser at 1123 nm with a Cr⁴⁺:YAG Saturable Absorber. *Appl. Phys. Express* **2011**, *4*, 092702. [[CrossRef](#)]
23. Chen, Y.F.; Lan, Y.P. Diode-pumped passively Q-switched Nd:YAG laser at 1123 nm. *Appl. Phys. B Lasers O* **2004**, *79*, 29–31. [[CrossRef](#)]
24. Huang, J.Y.; Liang, H.C.; Su, K.W.; Lai, H.C.; Chen, Y.F.; Huang, K.F. InGaAs quantum-well saturable absorbers for a diode-pumped passively Q-switched Nd:YAG laser at 1123 nm. *Appl. Opt.* **2007**, *46*, 239–242. [[CrossRef](#)] [[PubMed](#)]
25. Raikonen, E.; Kimmelma, O.; Kaivola, M.; Buchter, S.C. Passively Q-switched Nd:YAG/ICTA laser at 561 nm. *Opt. Commun.* **2008**, *281*, 4088–4091. [[CrossRef](#)]

26. Singh, S.; Smith, R.G.; Vanuiter, L. Stimulated-Emission Cross-Section and Fluorescent Quantum Efficiency of Nd³⁺ in Yttrium Aluminum Garnet at Room-Temperature. *Phys. Rev. B* **1974**, *10*, 2566–2572. [[CrossRef](#)]
27. Gao, C.; Wang, R.; Lin, Z.; Gao, M.; Zhu, L.; Zheng, Y.; Zhang, Y. 2 μm single-frequency Tm:YAG laser generated from a diode-pumped L-shaped twisted mode cavity. *Appl. Phys. B* **2012**, *107*, 67–70. [[CrossRef](#)]
28. Marling, J. 1.05-1.44 μm Tunability and Performance of CW Nd³⁺-YAG Laser. *IEEE J. Quant. Elect.* **1978**, *14*, 56–62. [[CrossRef](#)]
29. Barmenkov, Y.O.; Zalvidea, D.; Torres-Peiro, S.; Cruz, J.L.; Andres, M.V. Effective length of short Fabry-Perot cavity formed by uniform fiber Bragg gratings. *Opt. Express* **2006**, *14*, 6394–6399. [[CrossRef](#)] [[PubMed](#)]